Environmental Science & Technology

Article

Cite This: Environ. Sci. Technol. 2018, 52, 8977−8985

pubs.acs.org/est

Impact of Ohmic Resistance on Measured Electrode Potentials and Maximum Power Production in Microbial Fuel Cells

Bruce E. Logan,*[,†] Emily Zikmund,[†] Wulin Yang,[†] Ruggero Rossi,[†] Kyoung-Yeol Kim,[†] Pascal E. Saikaly,[‡] and Fang Zhang[§]

[†]Department of Civil and Environmental Engineering, The Pennsylvania State University, 231Q Sackett Building, University Park, Pennsylvania 16802, United States

[‡]Biological and Environmental Sciences and Engineering Division, Water Desalination and Reuse Research Center, King Abdullah University of Science and Technology, Thuwal 23955-6900, Saudi Arabia

[§]School of Environment and State Key Joint Laboratory of Environment Simulation and Pollution Control, Tsinghua University, Beijing 100084, China

Supporting Information

ABSTRACT: Low solution conductivity is known to adversely impact power generation in microbial fuel cells (MFCs), but its impact on measured electrode potentials has often been neglected in the reporting of electrode potentials. While errors in the working electrode (typically the anode) are usually small, larger errors can result in reported counter electrode potentials (typically the cathode) due to large distances between the reference and working electrodes or the use of whole cell voltages to calculate counter electrode potentials. As shown here, inaccurate electrode potentials impact conclusions concerning factors limiting power production in MFCs at higher current densities. To demonstrate how the electrochemical measurements should be adjusted using the solution conductivity, electrode potentials were estimated in MFCs with brush anodes placed close to the cathode (1 cm) or with flat felt anodes placed further from the cathode (3 cm) to avoid oxygen crossover to the anodes. The errors in the cathode potential for MFCs with brush anodes reached 94 mV using acetate in a 50 mM phosphate buffer solution. With a felt anode and acetate, cathode potential errors increased to 394 mV. While brush anode MFCs produced much higher power densities than flat anode MFCs under these conditions, this better performance was shown primarily to result from electrode spacing following correction of electrode potentials. Brush anode potentials corrected for solution conductivity were the same for brushes set 1 or 3 cm from the cathode, although the range of current produced was different due to ohmic losses with the larger distance. These results demonstrate the critical importance of using corrected electrode potentials to understand factors limiting power production in MFCs.

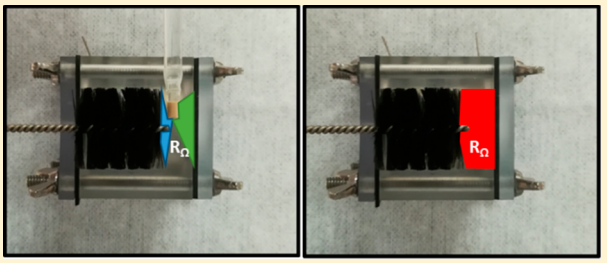

INTRODUCTION

Many different types of electrodes have been used in microbial fuel cells (MFCs) in order to try to increase power production.[1−9] Anodes such as graphite fiber brushes[10] or highly porous carbon felt[11,12] produce higher power densities in MFCs due to their high surface areas and porosities. A comparison of anode types based on reports in the literature showed that cylindrical brush anodes generally produced higher current densities than flat carbon felt, carbon cloth, and carbon paper anodes when coupled to a cathode with a platinum catalyst.[3] Placing the electrodes close to each other should improve power production as it reduces ohmic resistance. However, flat anodes cannot be placed close to the cathode unless a separator or membrane is used to block oxygen transfer from the cathode to the anode, as oxygen crossover reduces power production.[13−18] In contrast, a brush anode can be placed close to the cathode in the absence of a separator without an appreciable loss in power, as long as the brush is more than ∼1 cm thick.[10,19−22] The brush is quite thick relative to many felt or cloth anodes, which should facilitate maintenance of anaerobic conditions within the brush. Removing up to 65% of a 2.5 cm long brush on the side most distant from the cathode, so that the brush was only 0.9 cm thick, did not impact power production, suggesting that the portion of the anode closest to the cathode was important for power production.[19] Small diameter brushes (0.8 cm) have produced higher power densities than larger brushes (2.5 cm diameter) when acetate concentrations were kept high (∼1 g/L), but they have failed to produce stable power with lower strength wastewater (<0.3−0.6 g-COD/L).[20,22] Thus, the type

Received: April 17, 2018
Revised: June 5, 2018
Accepted: July 2, 2018
Published: July 2, 2018

DOI: 10.1021/acs.est.8b02055
Environ. Sci. Technol. 2018, 52, 8977−8985

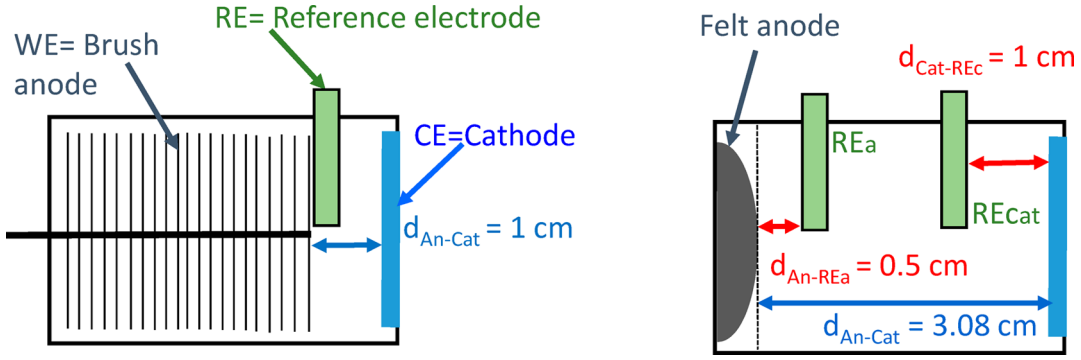

Figure 1. Schematics of different types of MFCs: (a) brush anode MFC with the RE placed inside the electric field and <0.2 cm distance from the working electrode (WE, brush anode); (b) flat felt anode MFC, which shows the felt slightly bowed outward due to the gasket holding it against the side of the MFC, with two REs inside the electric field. The dashed line indicates the distances relative to the anode for the REs and cathode.

and thickness of the anode can be factors affecting power production.

Accurate measurement of the electrode potentials is important for knowing how changes in electrode materials or electrode spacing alter performance. For example, if flat or thin anodes are placed too close to the cathode, oxygen contamination from the cathode can raise the anode potential and result in lower power production despite low ohmic resistances.[14,22] Many studies have shown in acetate-fed MFCs that the cathode potential decreases more rapidly with current than the brush anode potential, which indicated that the cathode was limiting power production.[23−26] In wastewater-fed MFCs, where the solution conductivity and substrate concentration (based on chemical oxygen demand, COD) are very low, the anode can also limit power production.[27] However, conclusions concerning which electrode limits power production require accurate measurements of the electrode potentials, particularly at higher current densities in solutions with low conductivities.

The distances between reference electrodes (REs) and working electrodes are usually not reported, confounding an analysis to calculate true electrode potentials. From an electrochemical perspective, the RE should be placed as close as possible to the working electrode, but when using a brush anode, it is not clear what portion of the brush surface should be used. For example, should the RE be placed near the brush surface (fibers) or near the metal current collector core? It is recommended that very small, Luggin-type electrodes be used,[28,29] but larger REs (~0.5 cm) are often used in MFC studies,[30,31] and it is not clear if placement of these larger electrodes in the current path impedes ion transfer and adversely impacts the electric field between the electrodes. When using flat anodes, REs commonly used in 4 cm cube reactors are typically inserted through a rubber stopper and are ~1 cm from a flat electrode.[12,32] A low conductivity solution, such as wastewater, will have a high ohmic resistance, and thus any appreciable distance between the RE and working electrode (if not compensated for using certain potentiostat software) can result in inaccurate measured potentials. In an MFC with a single RE, the cathode potential is often calculated as the difference between the anode potential and the whole cell potential.[12,33] However, the reported cathode potential using this approach will be wrong because it includes ohmic resistance between the two electrodes, producing a more negative potential than the actual cathode potential. These errors in the electrode potentials become larger as the current increases, as the ohmic resistance (R_Ω) is dependent on the current,[34] according to

$$E_{cell} = E_{emf} - \left(\sum \eta_a + |\sum \eta_c| + iR_\Omega\right) \quad (1)$$

where E_{cell} is the recorded cell voltage, E_{emf} is the electromotive force generated by the chemical reaction, η_a is the anode overpotential, η_c is the cathode overpotential, and i is the current. The electrode overpotentials include activation losses, bacterial metabolic losses, pH changes, and concentration losses due to insufficient chemical transport to or from the electrodes.[34,35] Thus, errors can be introduced into the measured electrode potentials due to ohmic losses included in the anode potential measurements and inclusion of ohmic losses between the electrodes into the calculated cathode potentials. While the importance of ohmic losses has been noted by some authors,[36] specific guidance on how to correct electrode potentials has not been previously reported in the bioelectrochemical literature.

In order to ensure more accurate reporting of electrode potentials, we developed a series of equations to explicitly show how electrode potentials can be corrected, as how maximum power densities are impacted by solution ohmic resistance. The resistances needed to make these adjustments can be obtained either from simply measuring the distances between electrodes and using the solution conductivity or by using a more advanced approach such as electrochemical impedance spectroscopy (EIS). The use of these equations was demonstrated here using electrode potentials and power densities obtained for MFCs with graphite fiber brush anodes or flat carbon felt anodes. The calculation of cathode potentials, when only a single RE was used, was shown to be particularly important for assessing how overpotentials changed at higher current densities. We assessed the impact of the placement of the RE inside and outside the current path using direct measurements of electrode spacing and calculations of ohmic resistance based on the conductivity of the solution. Different distances are often used between the anode and the cathode, and a flat anodes placed near the cathode can have a different potential than the same anode placed further from the anode due to oxygen crossover from the cathode. It is shown here using brush anodes, which are not adversely impacted by oxygen crossover when substrate concentrations do not limit anode performance, that when brush anode potentials are correctly reported, the distance between the anode and cathode does not impact anode potentials as a function of current density.

DOI: 10.1021/acs.est.8b02055
Environ. Sci. Technol. 2018, 52, 8977−8985

METHODS

MFC Configuration and Operation. MFCs were made from polycarbonate blocks drilled to contain a 3 cm diameter chamber that was 4 cm long (working volumes of 28 mL) as previously described.[37] Two anodes were used: brush anodes and flat anodes. Brush anodes were made from carbon fibers (PANEX 33 160 K, ZOLTEK) twisted between two titanium wires and were 2.5 cm long and 2.5 cm in diameter.[10] Flat anodes were made from 0.64 cm thick carbon felt (99% porosity, Alfa Aesar, Ward Hill, MA) cut slightly larger than 3 cm to expose 7 cm^2 of projected surface area.[12] All anodes were heat treated at 450 °C for 30 min in a muffle furnace prior to use.[38] Cathodes (7 cm^2 exposed surface) were made from activated carbon and stainless steel mesh, with a cathode specific surface area per volume of reactor of 25 m^2/m^3 (4 cm long MFC).[39] Cathodes for all tests conducted here were manufactured by VITO (Mol, Belgium) with a 70% porosity diffusion layer,[40,41] except as noted. For one analysis conducted here using brush anodes and wastewater, the cathodes were made using a hot press process with the activated carbon treated using a Fe−N−C compound to improve power production, as previously reported.[33]

Brush anodes were placed near the cathode (d_{An-Cat} = 1 cm, except as noted) so that the circular end of brush pointed was facing the cathode, with the RE tip set <0.2 cm above the wire center (d_{An-RE} = 0.2 cm) (Figure 1). In one set of experiments where the impact of solution resistance was examined, the length of the MFC was extended with an additional 2 cm cube so that the edge of the brush cathode was 3 cm from the cathode (d_{An-Cat} = 3 cm). Flat anodes were placed on the side opposite from the cathode to avoid oxygen contamination of the anode, with an estimated distance of d_{An-Cat} = 3.1 cm for the edge-to-edge distances at the middle of the electrodes, considering a slight bowing out of the anode toward the cathode (Figure 1). The center of one reference electrode placed 0.5 cm from the felt anode (d_{An-REa} = 0.5 cm), and the second reference electrode was placed 1.0 cm from the cathode ($d_{Cat-REc}$ = 1.0 cm). The REs used to measure electrode potentials (Ag/AgCl; model RE-5B, BASi, IN; +0.209 V versus a standard hydrogen electrode, SHE) were placed in the current path between the electrodes. The RE was 0.5 cm in diameter, with a tip diameter of 0.4 cm. Distances are considered to be accurate within 0.2 cm.

All tests conducted with sodium acetate (1 g/L) were conducted using a medium containing a 50 mM phosphate buffer solution (PBS; 4.58 g of Na_2HPO_4, 2.45 g of NaH_2PO_4, 0.31 g of NH_4Cl, 0.13 g of KCl in 1 L of distilled water, with 12.5 mL of a concentrated trace mineral solution and 5 mL of a vitamin solution).[3,42] Solution conductivity was measured for each EIS test as indicated, with variations in the range of 7.20−7.48 mS/cm. MFCs were inoculated using effluent from other operating acetate-fed MFCs and acclimated over multiple cycles until at least three reproducible voltage profiles were obtained. Data for tests with domestic wastewater, previously reported in terms of unadjusted electrode potentials, were reanalyzed to assess corrected cathode potentials and ohmic losses due to the low wastewater conductivity (~1.5 mS/cm).[14,33]

The ohmic resistances for a two electrode (anode and cathode) or a three-electrode (RE and felt or brush anode) setup were measured using electrochemical impedance spectroscopy (EIS) with a potentiostat (VMP3Multichannel Workstation, Biologic Science Instruments, USA).[43] EIS was performed over a frequency range of 100 kHz−5 mHz with sinusoidal perturbation of 10 mV amplitude, in a constant temperature room (30 °C). The set potentials for each experiment are given in the Supporting Information. The ohmic resistance was obtained from a Nyquist plot as the first x-intercept (lower value of x) in the high frequency range.

Estimating Ohmic Resistance from Solution Conductivity. The solution ohmic resistance per unit length, or R_Ω/l (Ω/cm), can be obtained from the measured solution conductivity (σ, mS/cm), as

$$\frac{R_\Omega}{l} = \frac{10^3}{\sigma A} \tag{2}$$

where A is the cross-sectional area (7 cm^2), and 10^3 is to convert mS into S (where 1 S = Ω^{-1}). The actual ohmic resistance can be measured using the current interrupt method or EIS,[34,44] but only if the reference electrode is in the electric field (i.e., between the anode and cathode).[45] The ohmic resistance estimated from the solution conductivity could underestimate the actual ohmic resistance as this approach does not include additional resistances at the electrode surface (or inside the brush or felt structure). Thus, a comparison of ohmic resistances based on both electrode spacing and EIS provides a method to assess possible inaccuracies based on estimated electrode distances and solution conductivity. The use of EIS is also required for correcting electrode potentials if separators or ion exchange membranes are placed between any two electrodes as this resistance is not included in the solution resistance, but it does contribute to ohmic resistance.

Electrode Potentials Using One RE. In many MFC studies, only one RE is used to report electrode potentials. If there is appreciable distance between the working electrode and the RE, which is often the case, then the measured electrode potential will include ohmic drop due to ohmic resistance, which is a function of current. Let us assume that the working electrode is the anode. The anode potential corrected for the ohmic resistance using a single RE (E_{AnRE}, mV) can be estimated using the measured potential (E_{An}, mV) as

$$E_{AnRE} = E_{An} - \left(\frac{10^3 R_\Omega d_{An-RE}}{l}\right) i \tag{3}$$

where d_{An-RE} is the distance (cm) between the anode and the RE and i is the current (A) (Figure 1). If a potentiostat is used, then it may have software that can automatically correct the anode potential for ohmic resistance, which would result in $E_{AnRE} = E_{An}$.

The cathode potential ($E_{Cat,U}$, mV) is sometimes incorrectly calculated from the uncorrected anode potential and the measured whole cell voltage (U, mV)[33,46,47] as

$$E_{Cat,U} = E_{An} + U \tag{4}$$

Unfortunately, eq 4 contains two errors which have not been previously noted: the use of an incorrect anode potential if the potential is not corrected for the loss due to the ohmic resistance of the solution in the gap between the anode and RE and using U because the measured U includes the potential lost due to the ohmic resistance of the solution between the anode and cathode. The first error in the cathode potential can be avoided by using the corrected anode potential eq 3 as

DOI: 10.1021/acs.est.8b02055
Environ. Sci. Technol. 2018, 52, 8977−8985

$$E_{Cat,U+AnRE} = E_{AnRE} + U \quad (5)$$

The result of this adjustment is that the corrected cathode potential will be equal to or more positive than that calculated using eq 4. The second error in eq 4 due to the use of U can be avoided by adding the potential lost by the current-dependent whole cell ohmic drop due to ohmic resistance, based on the distance between the electrodes (d_{An-Cat}), as

$$E_{Cat,U+AnRE+IR} = E_{AnRE} + U + \left(\frac{10^3 R_\Omega d_{An-Cat}}{l}\right) i \quad (6)$$

Thus, eq 6 provides a better approach to correct the cathode potential when only one RE is used with the anode as the working electrode.

An alternative approach to calculate the cathode potential using one RE is to use the cathode as the working electrode when obtaining polarization data. In that case, the cathode potential would be calculated using eq 3 for the cathode potential, with the distance between the cathode and RE defined as d_{Cat-RE}.

The correct distances to use for these equations, such as the electrode spacing distance (d_{An-Cat}) in eq 6, can be difficult to estimate for large and highly porous electrodes, such as graphite fiber brush electrodes or thick carbon felt, as it is not clear whether the distance should be from the edge of the electrode or the middle of the electrode (Figure 1). For all calculations here, we used the distance between the closest edges of the anode and cathode.

Electrode Potentials Using Two REs. Instead of estimating the cathode potentials based on a single RE, if there is sufficient space between the electrodes it is possible to use two REs: one placed close to the anode (REa) and one placed close to the cathode (REc) (Figure 1). The current-dependent corrected anode (E_{AnREa}, mV) and cathode potentials (E_{CatREc}, mV) can be calculated as

$$E_{AnREa} = E_{An} - \left(\frac{10^3 R_\Omega d_{An-REa}}{l}\right) i \quad (7)$$

$$E_{CatREc} = E_{Cat} + \left(\frac{10^3 R_\Omega d_{Cat-REc}}{l}\right) i \quad (8)$$

where d_{AnREa} is the distance (cm) between the anode and the anode reference electrode, E_{Cat} is the measured cathode potential, and $d_{Cat-REc}$ is the distance between the cathode and the cathode reference electrode. If the solution conductivity and distances between electrodes are all correct, the cathode potentials estimated using one RE (eq 6) should be the same as those obtained using two REs with eq 8.

Power Densities. The power produced by an MFC (P_p, W/m^2), normalized by the cathode projected surface area (assumed to be the same as the cross-sectional area, or $A_{cat} = A$), is obtained from the whole cell voltage (U, mV), based on using a resistor of R_{ex} in the circuit, as

$$P_p = \frac{10Ui}{A_{Cat}} = \frac{U^2}{100 A_{Cat} R_{ex}} \quad (9)$$

A plot of the power as a function of the current, called the power density curve, will typically produce a bell-shaped curve having a maximum power (P_{max}). The power that is lost due to the ohmic resistance of the solution (P_Ω) between the electrodes (due to the space between the anode and cathode) as a function of the current can be estimated as

$$P_\Omega = \frac{10^4 R_\Omega d_{An-Cat} i^2}{l A_{Cat}} \quad (10)$$

The sum of the power produced and the power lost to ohmic resistance ($P_{p+\Omega}$) is

$$P_{p+\Omega} = P_p + P_\Omega \quad (11)$$

Equation 11 helps to assess the impact of ohmic losses on power generation for the given conditions.

The maximum power in an MFC with high ohmic resistance typically occurs at about 1/2 the maximum current ($^1/_2 i_{max}$), and a voltage of less than 1/2 of the open circuit voltage ($^1/_2 U_{OC}$, mV), for bell-shaped power density curves. If internal resistance lost is assumed to be only due to ohmic resistance (eq 1), we can estimate the maximum current from a reduction of the voltage ($i_{max,\Omega}$) due to ohmic losses between the electrodes using Ohm's law as

$$i_{max,\Omega} = \frac{U_{OC} l}{10^3 R_\Omega d_{An-Cat}} \quad (12)$$

The maximum power that can be obtained with this ohmic drop between the electrodes ($P_{max,\Omega}$) can be estimated as the product of $^1/_2 i_{max,\Omega}$ and $^1/_2 U_{OC}$ or

$$P_{max,\Omega} = \frac{10 U_{OC} i_{max,\Omega}}{4 A_{Cat}} \quad (13)$$

For example, if R_Ω/l = 20 Ω cm^{-1} and d_{An-Cat} = 1 cm, for U = 492 mV, the maximum possible power density is 4.39 W m^{-2} (Supporting Information, Figure S1).

When both the anode and cathode potentials are measured, the power that could be produced based on these potentials, neglecting ohmic resistance between the electrodes, could be calculated using

$$P_{Cat-An} = \frac{10(E_{cat} - E_{An}) i}{A_{Cat}} \quad (14)$$

However, eq 14 includes errors in the measured electrode potentials primarily due to ohmic losses between the working and reference electrodes, and it does not account for ohmic losses between the electrodes which would prevent this level of power production. If the corrected electrode potentials are used, and the power due to ohmic losses for this potential difference and current density are included in this calculated power, then the total power can be better approximated as

$$P_{CatREc-AnREa-IR} = \left[E_{CatREc} - E_{AnREa} - \left(\frac{R_\Omega d_{An-Cat}}{l}\right) i\right] \frac{10i}{A_{cat}} \quad (15)$$

If all ohmic losses are correctly estimated, then the power calculated using eq 15 should be equal to that determined by the voltage over an external resistor using eq 9.

RESULTS AND DISCUSSION

Ohmic Losses and Power Densities in Brush Anode MFCs with 50 mM PBS. For the brush anode MFCs with the RE placed close to the anode (working electrode), there was little impact on the measured anode potentials due to the close spacing of the RE and working electrodes (<0.2 cm) (Figure

DOI: 10.1021/acs.est.8b02055
Environ. Sci. Technol. 2018, 52, 8977−8985

2A). For a solution conductivity of 7.2 mS/cm, a 0.2 cm distance is equivalent to a solution resistance of 4 Ω (eq 2). At

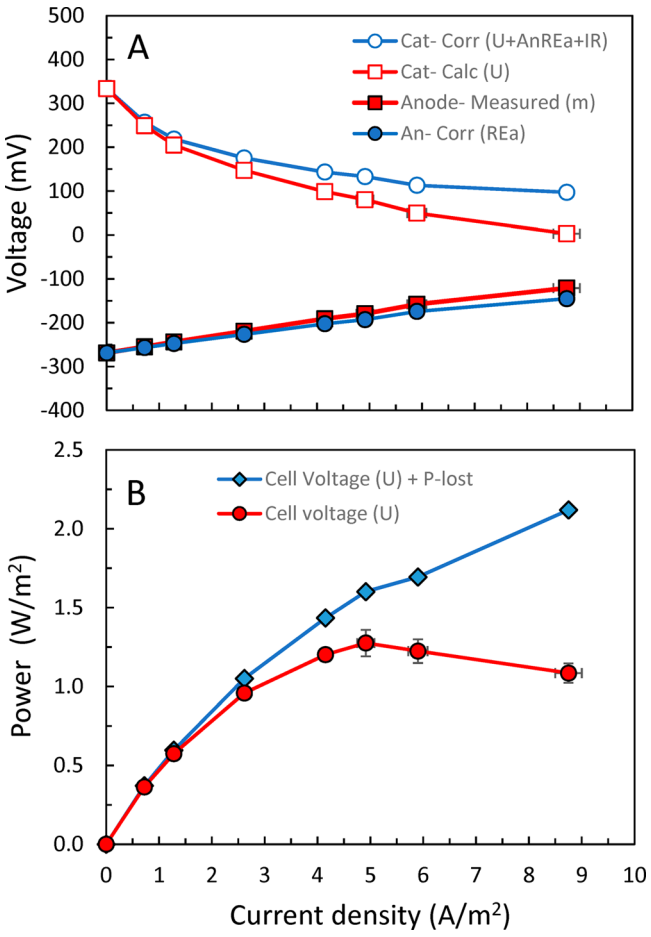

Figure 2. Brush anode MFCs with acetate and 50 mM PBS with a single RE. (A) Electrode potentials with and without ohmic resistance corrections. Anode measured (m) or corrected (REa, eq 7) using the RE. Cathode calculated using U (eq 4) or also calculated using the corrected anode potential and including the ohmic resistance (U +AnREa+IR, eq 6). (B) Power density curves based on measured cell voltage (U, eq 9) or with the added power lost due to ohmic resistances (cell voltage (U) + P-lost, eq 11).

the maximum current produced in these tests, the largest difference between the measured and corrected anode potentials due to the solution resistance was −24 mV (eq 3). Much larger errors were contained in the cathode potentials calculated using the measured anode potential and whole cell voltage (eq 4), with a difference of up to 94 mV at the highest current density of 8.8 A/m^2. The position of the RE relative to the brush did not impact the measured potentials when it was placed close to the anode. When the RE was moved upward or downward toward the core wire (with the RE in the electrical field), or when the RE was set above the anode (but still close to its surface), the anode potentials were unchanged.

Based on the change in the electrode potentials with current, both electrodes showed substantial overpotentials, but primarily the cathode limited power production based on a large change in electrode potential. With uncorrected potentials, there was a larger apparent drop in cathode potential (331 mV) compared to the anode potential (148 mV) at the highest current density (8.8 A/m^2) (Figure 2A). Even after correcting the electrode potentials, the change in cathode potential was still much larger (237 mV) than that of the anode (124 mV), indicating the larger impact of cathode performance on the power produced in this MFC.

The maximum measured power density for the brush anode MFCs (eq 9) was 1.28 ± 0.08 W/m^2 (Figure 2B). This maximum compares favorably to the range of power densities typically obtained in our laboratory using these reactors and solutions (1.36 ± 0.20 W/m^2).[3] Ohmic losses due to the solution resistance at the point of maximum power accounted for a loss of power of 0.33 W/m^2 (eq 10), which was 35% of the sum of the power in the circuit or lost to solution resistance (1.69 W/m^2) at a current of 4.9 A/m^2 (eq 11). These are all much less than the maximum possible power density of 6.7 W/m^2 in this system based on the measured OCV (603 mV) and the estimated maximum current (45 A/m^2) due to for the given electrode spacing and solution resistance (eq 13).

The distances between the electrodes were estimated based on the placement of the electrode and compared to those calculated on the basis of the measured ohmic resistances using EIS and the solution conductivity. Placement of the RE or distances measured using a ruler could not be set accurately to more than 0.2 cm, and with this margin of error, all distances were in good agreement by the two methods. For the brush anode MFCs (two electrode setup), the estimated distance between the edge of the brush and the cathode was estimated as 1 cm, with d_{An-Cat} = 0.97 cm obtained from on EIS measurements (Figure S3).

Ohmic Losses and Power Densities in Felt Anode MFCs with 50 mM PBS. When felt anodes were used in the MFCs, larger distances were used between the RE and working electrodes compared to the brush anode configuration in order to avoid oxygen contamination of the anode. For these test conditions, the main impact on performance was this large distance between the anode and cathode, with a maximum current density of 4.7 A/m^2 (Figure 3). The ohmic loss between the anode and RE of 34 mV (Figure 3A) was larger than that produced with the brush anode (24 mV) (eq 3), despite lower current densities, due to the greater RE−anode estimated distance for the felt anode (d_{An-Cat} = 0.5 cm). The ohmic correction needed for the cathode potential based on measurement using the second RE reached a maximum of 68 mV at the highest current density. However, if the cathode potential had been reported using the measured anode potential and the whole cell voltage (eq 4), the cathode potential at the highest current density would have been −46 mV, which would be an error of 209 mV compared to the cathode potential of 141 mV using the RE and the solution resistance (Figure 3A)

The maximum measured power density for the felt MFC was 0.71 ± 0.06 W/m^2 (eq 9), with the power lost to ohmic resistances at the corresponding current density (3.19 A/m^2) contributing 0.43 W/m^2, or a total of 38% of the sum of the power produced and lost to ohmic resistance of 1.14 W/m^2 (Figure 3B). Using the measured electrode potentials (no corrections for ohmic losses between the REs), the estimated power without consideration of the large ohmic losses between the electrodes would have been 0.94 W/m^2 (eq 14). With the large electrode spacing of 3.1 cm, only a maximum of 2.3 W/m^2 would be possible in this configuration based on the large ohmic resistance and the OCV (eq 13). While power could

DOI: 10.1021/acs.est.8b02055
Environ. Sci. Technol. 2018, 52, 8977−8985

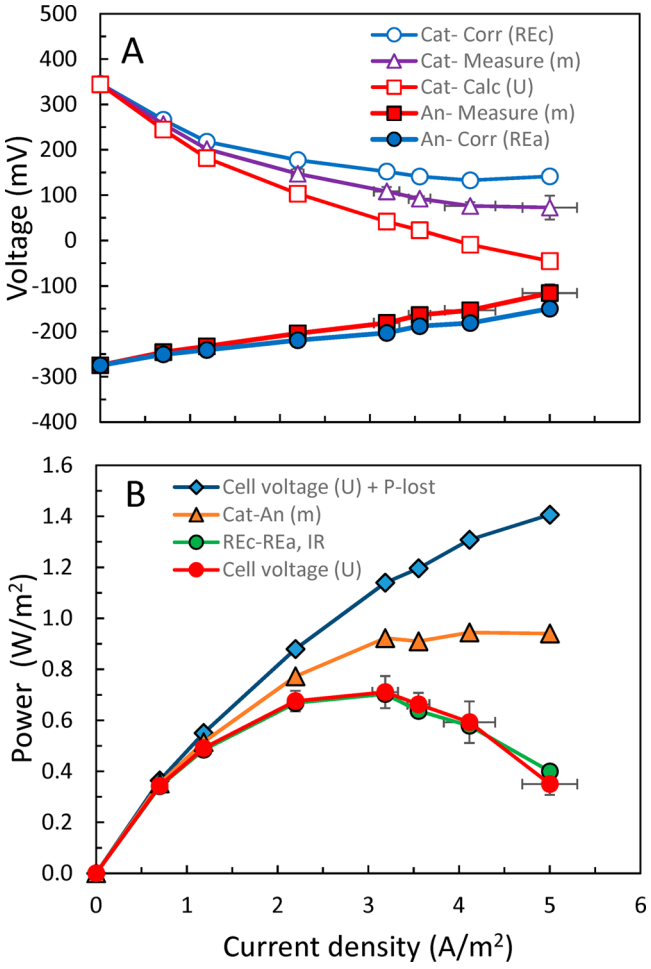

Figure 3. Felt anode MFCs with acetate and 50 mM PBS, with two REs. (A) Electrode potentials with and without ohmic resistance corrections. Anode measured (m) or corrected (REa, eq 7) using the RE near the anode. Cathode calculated using U (eq 4) or measured using the RE near the cathode (m) or corrected (REc, eq 8) using the RE near the cathode. (B) Power density curves based on measured cell voltage (U, eq 9) or with other corrections: using the electrode potentials corrected for ohmic drop between the RE and the electrode, but considering ohmic losses for the anode−cathode spacing (REc−REa, IR, eq 15); using the measured electrode potentials (Cat−An (m), eq 14); and using the cell voltage and the power lost due to ohmic resistances (cell voltage (U) + P-lost, eq 11).

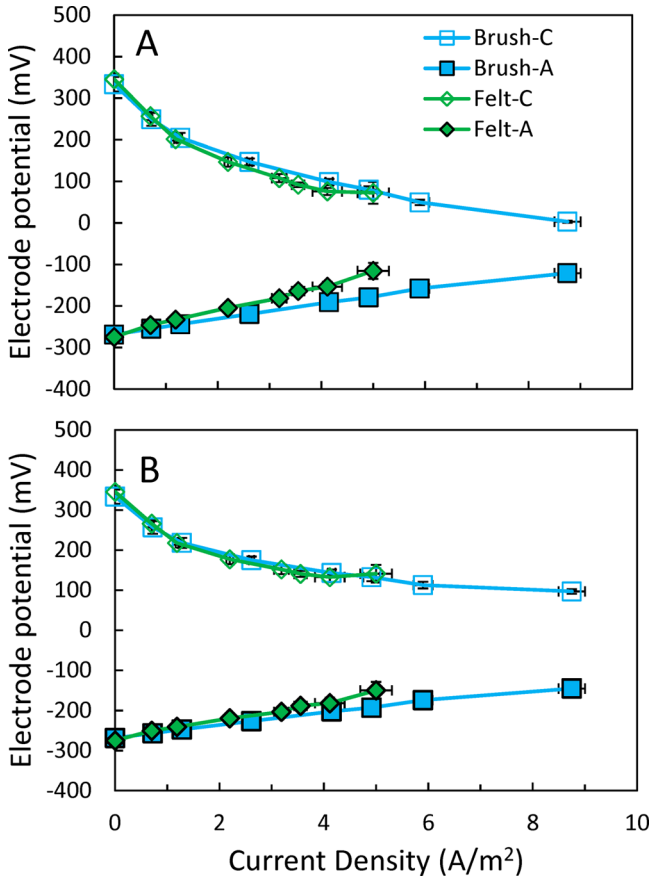

Figure 4. Comparison of the electrode potentials for the brush anode MFC, for the cathode (Brush-C) or anode (Brush-A), and for the felt anode MFC, for the cathode (Felt-C) and anode (Felt-A), using a single RE in each MFC: (A) using the measured anode potential and calculating the cathode potential from the cell voltage (eq 3) and (B) using the corrected anode potentials and the measured cathode potential for the felt anode MFC (eq 7) and the cathode potential corrected for the ohmic resistance (eq 5).

have theoretically been higher by using a smaller electrode spacing, it has been well shown that power would actually decrease in the absence of a separator due to oxygen crossover from the cathode to the anode.[14,48]

For felt anode MFCs, we estimated an anode-to-cathode distance of 3.1 cm (less than 4 cm due to the thickness of the felt anode and a bowed-out shape due to the gasket holding the anode), with an average based on EIS measurements of d_{An-Cat} = 3.08 cm (Figure S4). The RE and working electrode distances (three-electrode setup) for the brush anode MFCs were <0.2 cm estimated to the anode, with a measured distance of d_{An-RE} = 0.08 cm, and 1.0 cm to the cathode, with a calculated distance using EIS of d_{Cat-RE} = 0.97 cm (Figures S5 and S6). For the felt anode MFCs, the estimated and measured RE to electrode distances were 0.5 cm estimated to the anode, with a measured distance of using EIS of 0.51 cm, and 1.0 cm to the cathode, with a measured distance of using EIS of 0.97 cm (Figures S7 and S8).

Comparison of Brush and Felt Potentials in 50 mM PBS. The relative performance of the brush and felt anodes was compared based on using the uncorrected and corrected electrode potentials over the range of measured current densities (Figure 4). The cathode potentials were essentially identical to each other for the brush and felt MFCs, both before and after correction for the ohmic losses between the reference electrodes, with the main difference being the range of the current densities was higher using the brush anodes. For the anode potentials, however, there were appreciable differences before correction measurements for the distances between the anode and RE (Figure 4A). Even after correcting for this ohmic loss, there were still noticeable differences between the anode potentials at the higher current densities for the felt anode (Figure 4B), suggesting the brush anode did improve performance. To demonstrate that the impact of electrode spacing was not a factor in the difference between the brush and felt anodes, additional tests were conducted with the edge of the brush anode moved to be 3 cm from the cathode. The anode and cathode potentials measured were identical using two REs placed close to the electrodes for the 3 cm

DOI: 10.1021/acs.est.8b02055
Environ. Sci. Technol. 2018, 52, 8977−8985

electrode spacing, to that obtained using one RE placed close to the anode and a 1 cm electrode spacing, but the power density decreased substantially from 1.26 ± 0.05 to 0.89 ± 0.01 W m^{-2} (Figure S9). Based on the changes in potentials with and without correction of the potentials, and small differences between the brush and felt anodes, the greatest impact on power production was not the type of anode but the distances between the electrodes.

Ohmic Losses and Power Densities in Brush Anode MFCs with Domestic WW. Power production using domestic wastewater is challenging due to its low solution conductivity. For example, the ohmic loss due to a 1 cm anode−cathode spacing is 95 Ω for wastewater with a conductivity of 1.5 mS/cm, or 143 Ω for a conductivity of 1 mS/cm, compared to 20 Ω for 50 mM PBS (~7 mS/cm) (eq 2). The highest power density produced using domestic wastewater in our laboratory of 0.80 ± 0.03 W/m^2 was obtained using brush anodes (1 cm electrode spacing) and activated carbon cathodes modified using an Fe−N−C compound.[33] At the highest current density of 3.8 A/m^2, the reported difference in electrode potential was 153 mV, and the system appeared to suffer from both anode and cathode limited power generation.

Further analysis of that data using wastewater and Fe−N−C/activated carbon cathodes,[33] by correcting the electrode potentials for ohmic resistances, showed a much greater difference in electrode potentials (278 mV) than that reported in the original study (153 mV) at the highest current density of 3.76 A/m^2 (Figure 5A). An important trend that was revealed after using the corrected data is that the cathode potentials leveled off at the higher current densities, while the anode potential continued to rise at approximately the same rate over the range of current densities (Figure 5A). This continued rise of the anode potential indicated that the anode was primarily limiting power production, with an overall loss of potential for the anode of 99 mV, compared to only 47 mV for the cathode, at current densities >2.4 A/m^2 (after the peak power). The maximum power density possible based on 1 cm electrode spacing, the measured open circuit potential, and the ohmic resistance of the wastewater is 4.7 W/m^2 (eq 13), but this would never be achieved due to the rapid drop-off in electrode potentials.

Implications for MFC Performance. In most MFC studies the distances between the RE and working electrodes, or the method to calculate the cathode potentials, have not been reported.[33,46,47] Even small distances in low conductivity solutions like wastewaters can lead to substantial errors between the reported anode potential and RE. However, the largest errors have likely resulted in the reported cathode potentials when the whole cell voltages have been used to calculate cathode potentials with only a single RE and the anode as the working electrode. As shown here, the solution conductivity can be used to estimate the ohmic resistance just based on measured spacing between the RE and a working electrode or the distance between the anode and cathode, as the ohmic resistances obtained from measured distances agreed well with measurements made using EIS. When the cathode potential was adjusted for ohmic resistance, it was demonstrated in tests with domestic wastewater that the anode potential was limiting power production. Using the single RE and making the anode or cathode the working electrode also provides a suitable method to report the cathode potentials if ohmic losses are corrected between the working electrode and the RE, but it is not clear that this has been correctly done in previous studies.

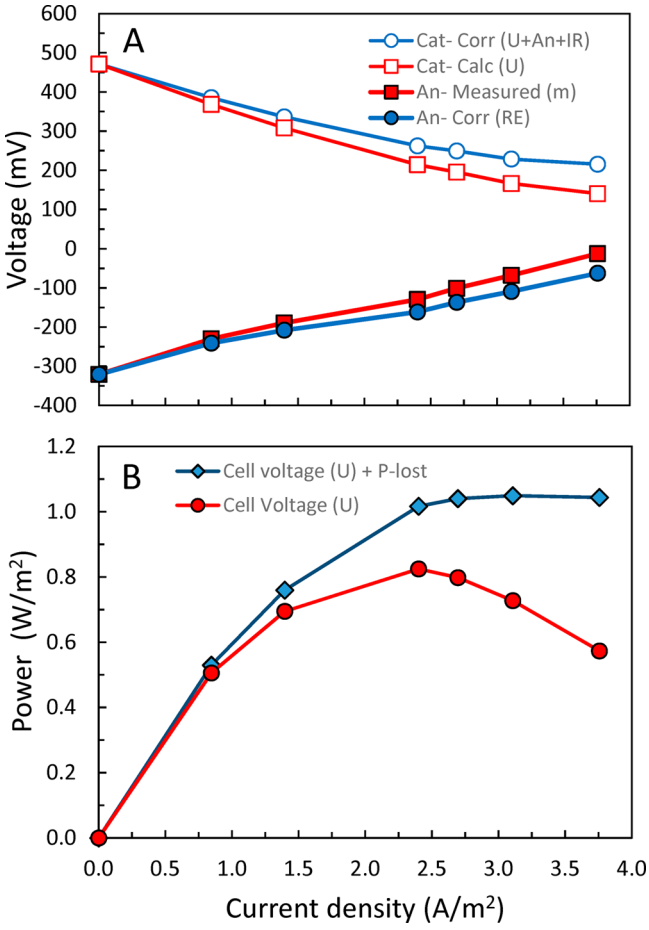

Figure 5. Brush anode MFCs with domestic wastewater and a single RE. (A) Electrode potentials with and without ohmic resistance corrections. Anode measured (m) or corrected (REa, eq 7) using the RE. Cathode calculated using U (eq 4) or also calculated using the corrected anode potential and including the ohmic resistance (U +AnREa+IR, eq 6). (B) Power density curves based on measured cell voltage (U, eq 9) or with the added power lost due to ohmic resistances (Cell voltage (U) + P-lost, eq 11). (Uncorrected data are from Yang and Logan.[33])

The use of the adjusted potentials provides an approach to estimate limits on MFC performance based on electrode potentials in the presence or absence of ohmic resistance. For example, MFCs with flat anodes produced 0.71 ± 0.06 W/m^2, with a maximum of 2.3 W/m^2 possible based on the open circuit voltage and the solution conductivity for 50 mM PBS with acetate. However, due to the large electrode spacing of 3.1 cm, the power lost to ohmic resistances were 0.43 W/m^2 even with 50 mM PBS (eq 10). Brush and flat felt anodes produced similar OCVs, and thus in theory they could produce similar power densities at similar anode−cathode spacing. Brush anodes can be placed closer to the cathode than felt anodes, as they are not impacted by oxygen crossover from the cathode, and therefore this reduced spacing enables higher power production. As a result of reduced electrode spacing, and slightly more negative potentials at current densities similar to felt anodes, brush anodes produced about twice the power (1.28 ± 0.08 W/m^2) than flat anodes, with a maximum possible power density of the brush anodes of 6.7 W/m^2 in 50

DOI: 10.1021/acs.est.8b02055
Environ. Sci. Technol. 2018, 52, 8977−8985

mM PBS. Thus, brush anodes continue to be recommended for use in MFCs primarily due to less ohmic losses when they are placed closer to the cathode. Estimation of maximum power densities for both types of cathodes will require more accurate measurements of electrode potentials and electrode spacing, especially for low conductivity solutions such as domestic wastewaters.

■ ASSOCIATED CONTENT

Supporting Information

The Supporting Information is available free of charge on the ACS Publications website at DOI: 10.1021/acs.est.8b02055.

Calculations and figures showing polarization and power density curves for a MFCs limited by ohmic resistance or internal resistance, six figures showing ohmic resistance determined using electrochemical impedance spectroscopy, and a figure showing a comparison of electrode potentials using brush or felt anodes (PDF)

■ AUTHOR INFORMATION

Corresponding Author

*(B.E.L.) E-mail blogan@psu.edu; Ph +1-814-863-7908; Fax +1 814 863-7304.

ORCID

Bruce E. Logan: 0000-0001-7478-8070

Kyoung-Yeol Kim: 0000-0002-2655-7806

Notes

The authors declare no competing financial interest.

■ ACKNOWLEDGMENTS

The research was supported by funds provided by the National Renewable Energy Laboratory (NREL) through the Department of Energy (DOE) CPS Project #21263, and the Environmental Security Technology Certification Program via cooperative research agreement W9132T-16-2-0014 through the US Army Engineer Research and Development Center.

■ REFERENCES

(1) Kumar, G. G.; Sarathi, V. G. S.; Nahm, K. S. Recent advances and challenges in the anode architecture and their modifications for the applications of microbial fuel cells. *Biosens. Bioelectron.* **2013**, *43*, 461−475.

(2) Wei, J.; Liang, P.; Huang, X. Recent progress in electrodes for microbial fuel cells. *Bioresour. Technol.* **2011**, *102*, 9335−9344.

(3) Yang, W.; Kim, K.-Y.; Saikaly, P. E.; Logan, B. E. The impact of new cathode materials relative to baseline performance of microbial fuel cells all with the same architecture and solution chemistry. *Energy Environ. Sci.* **2017**, *10*, 1025−1033.

(4) Mohanakrishna, G.; Krishna Mohan, S.; Venkata Mohan, S. Carbon based nanotubes and nanopowder as impregnated electrode structures for enhanced power generation: Evaluation with real field wastewater. *Appl. Energy* **2012**, *95*, 31−37.

(5) Baudler, A.; Schmidt, I.; Langner, M.; Greiner, A.; Schroder, U. Does it have to be carbon? Metal anodes in microbial fuel cells and related bioelectrochemical systems. *Energy Environ. Sci.* **2015**, *8*, 2048−2055.

(6) Valipour, A.; Ayyaru, S.; Ahn, Y. Application of graphene-based nanomaterials as novel cathode catalysts for improving power generation in single chamber microbial fuel cells. *J. Power Sources* **2016**, *327*, 548−556.

(7) Wang, H.; Ren, Z. J. A comprehensive review of microbial electrochemical systems as a platform technology. *Biotechnol. Adv.* **2013**, *31*, 1796−1807.

(8) Li, B.; Zhou, J.; Zhou, X.; Wang, X.; Li, B.; Santoro, C.; Grattieri, M.; Babanova, S.; Artyushkova, K.; Atanassov, P.; Schuler, A. J. Surface Modification of Microbial Fuel Cells Anodes: Approaches to Practical Design. *Electrochim. Acta* **2014**, *134*, 116−126.

(9) You, J.; Santoro, C.; Greenman, J.; Melhuish, C.; Cristiani, P.; Li, B.; Ieropoulos, I. Micro-porous layer (MPL)-based anode for microbial fuel cells. *Int. J. Hydrogen Energy* **2014**, *39*, 21811−21818.

(10) Logan, B. E.; Cheng, S.; Watson, V.; Estadt, G. Graphite fiber brush anodes for increased power production in air-cathode microbial fuel cells. *Environ. Sci. Technol.* **2007**, *41*, 3341−3346.

(11) Ge, B.; Li, K.; Fu, Z.; Pu, L.; Zhang, X.; Liu, Z.; Huang, K. The performance of nano urchin-like $NiCo_2O_4$ modified activated carbon as air cathode for microbial fuel cell. *J. Power Sources* **2016**, *303*, 325−332.

(12) Ahn, Y.; Logan, B. E. Altering anode thickness to improve power production in microbial fuel cells with different electrode distances. *Energy Fuels* **2013**, *27*, 271−276.

(13) Cheng, S.; Liu, H.; Logan, B. E. Increased power generation in a continuous flow MFC with advective flow through the porous anode and reduced electrode spacing. *Environ. Sci. Technol.* **2006**, *40*, 2426−2432.

(14) Hays, S.; Zhang, F.; Logan, B. E. Performance of two different types of anodes in membrane electrode assembly microbial fuel cells for power generation from domestic wastewater. *J. Power Sources* **2011**, *196*, 8293−8300.

(15) Fan, Y.; Han, S.-K.; Liu, H. Improved performance of CEA microbial fuel cells with increased reactor size. *Energy Environ. Sci.* **2012**, *5*, 8273−8280.

(16) Zhang, F.; Xia, X.; Luo, Y.; Sun, D.; Call, D. F.; Logan, B. E. Improving startup performance with carbon mesh anodes in separator electrode assembly microbial fuel cells. *Bioresour. Technol.* **2013**, *133*, 74−81.

(17) Zhang, X.; Cheng, S.; Huang, X.; Logan, B. E. The use of nylon and glass fiber filter separators with different pore sizes in air-cathode single-chamber microbial fuel cells. *Energy Environ. Sci.* **2010**, *3*, 659−664.

(18) Zhang, X.; Cheng, S.; Liang, P.; Huang, X.; Logan, B. E. Scalable air cathode microbial fuel cells using glass fiber separators, plastic mesh supporters, and graphite fiber brush anodes. *Bioresour. Technol.* **2011**, *102*, 372−375.

(19) Hutchinson, A. J.; Tokash, J. C.; Logan, B. E. Analysis of carbon fiber brush loading in anodes on startup and performance of microbial fuel cells. *J. Power Sources* **2011**, *196*, 9213−9219.

(20) Lanas, V.; Ahn, Y.; Logan, B. E. Effects of carbon brush anode size and loading on microbial fuel cell performance in batch and continuous mode. *J. Power Sources* **2014**, *247*, 228−234.

(21) Lanas, V.; Logan, B. E. Evaluation of multi-brush anode systems in microbial fuel cells. *Bioresour. Technol.* **2013**, *148*, 379−385.

(22) Stager, J. L.; Zhang, X.; Logan, B. E. Addition of acetate improves stability of power generation using microbial fuel cells treating domestic wastewater. *Bioelectrochemistry* **2017**, *118*, 154−160.

(23) Ahn, Y.; Ivanov, I.; Nagaiah, T. C.; Bordoloi, A.; Logan, B. E. Mesoporous nitrogen-rich carbon materials as cathode catalysts in microbial fuel cells. *J. Power Sources* **2014**, *269*, 212−215.

(24) Wang, L.; Liang, P.; Zhang, J.; Huang, X. Activity and stability of pyrolyzed iron ethylenediaminetetraacetic acid as cathode catalyst in microbial fuel cells. *Bioresour. Technol.* **2011**, *102*, 5093−5097.

(25) Lu, G.; Zhu, Y.; Lu, L.; Xu, K.; Wang, H.; Jin, Y.; Jason Ren, Z.; Liu, Z.; Zhang, W. Iron-rich nanoparticle encapsulated, nitrogen doped porous carbon materials as efficient cathode electrocatalyst for microbial fuel cells. *J. Power Sources* **2016**, *315*, 302−307.

(26) Nguyen, M.-T.; Mecheri, B.; Iannaci, A.; D'Epifanio, A.; Licoccia, S. Iron/polyindole-based electrocatalysts to enhance oxygen reduction in microbial fuel cells. *Electrochim. Acta* **2016**, *190*, 388−395.

(27) Ahn, Y.; Logan, B. A multi-electrode continuous flow microbial fuel cell with separator electrode assembly design. *Appl. Microbiol. Biotechnol.* **2012**, *93*, 2241−2248.

(28) Bard, A. J.; Faulkner, L. R. *Electrochemical Methods: Fundamentals and Applications*, 2nd ed.; John Wiley & Sons: New York, 2001.
(29) Santoro, C.; Kodali, M.; Kabir, S.; Soavi, F.; Serov, A.; Atanassov, P. Three-dimensional graphene nanosheets as cathode catalysts in standard and supercapacitive microbial fuel cell. *J. Power Sources* **2017**, *356*, 371−380.
(30) He, W.; Zhang, X.; Liu, J.; Zhu, X.; Feng, Y.; Logan, B. E. Microbial fuel cells with an integrated spacer and separate anode and cathode modules. *Environ. Sci. Water Res. Technol.* **2016**, *2*, 186−195.
(31) Yang, W.; Logan, B. E. Engineering a membrane based air cathode for microbial fuel cells via hot pressing and using multi-catalyst layer stacking. *Environ. Sci. Water Res. Technol.* **2016**, *2*, 858−863.
(32) Chen, Z.; Li, K.; Pu, L. The performance of phosphorus (P)-doped activated carbon as a catalyst in air-cathode microbial fuel cells. *Bioresour. Technol.* **2014**, *170*, 379−384.
(33) Yang, W.; Logan, B. E. Immobilization of a metal−nitrogen−carbon catalyst on activated carbon with enhanced cathode performance in microbial fuel cells. *ChemSusChem* **2016**, *9*, 2226−2232.
(34) Logan, B. E.; Aelterman, P.; Hamelers, B.; Rozendal, R.; Schröder, U.; Keller, J.; Freguia, S.; Verstraete, W.; Rabaey, K. Microbial fuel cells: methodology and technology. *Environ. Sci. Technol.* **2006**, *40*, 5181−5192.
(35) Hou, J.; Liu, Z.; Zhou, Y.; Chen, W.; Li, Y.; Sang, L. An experimental study of pH distributions within an electricity-producing biofilm by using pH microelectrode. *Electrochim. Acta* **2017**, *251*, 187−194.
(36) Harrington, T. D.; Babauta, J. T.; Davenport, E. K.; Renslow, R. S.; Beyenal, H. Excess surface area in bioelectrochemical systems causes ion transport limitations. *Biotechnol. Bioeng.* **2015**, *112*, 858−866.
(37) Liu, H.; Logan, B. E. Electricity generation using an air-cathode single chamber microbial fuel cell in the presence and absence of a proton exchange membrane. *Environ. Sci. Technol.* **2004**, *38*, 4040−4046.
(38) Feng, Y.; Yang, Q.; Wang, X.; Logan, B. E. Treatment of graphite fiber brush anodes for improving power generation in air-cathode microbial fuel cells. *J. Power Sources* **2010**, *195*, 1841−1844.
(39) Logan, B. E.; Wallack, M. J.; Kim, K.-Y.; He, W.; Feng, Y.; Saikaly, P. E. Assessment of microbial fuel cell configurations and power densities. *Environ. Sci. Technol. Lett.* **2015**, *2*, 206−214.
(40) Zhang, F.; Cheng, S.; Pant, D.; Bogaert, G. V.; Logan, B. E. Power generation using an activated carbon and metal mesh cathode in a microbial fuel cell. *Electrochem. Commun.* **2009**, *11*, 2177−2179.
(41) Zhang, F.; Pant, D.; Logan, B. E. Long-term performance of activated carbon air cathodes with different diffusion layer porosities in microbial fuel cells. *Biosens. Bioelectron.* **2011**, *30*, 49−55.
(42) Cheng, S.; Xing, D.; Call, D. F.; Logan, B. E. Direct biological conversion of electrons into methane by electromethanogenesis. *Environ. Sci. Technol.* **2009**, *43*, 3953−3958.
(43) ter Heijne, A.; Schaetzle, O.; Gimenez, S.; Navarro, L.; Hamelers, B.; Fabregat-Santiago, F. Analysis of bio-anode performance through electrochemical impedance spectroscopy. *Bioelectrochemistry* **2015**, *106*, 64−72.
(44) Bonanni, P. S.; Schrott, G. D.; Robuschi, L.; Busalmen, J. P. Charge accumulation and electron transfer kinetics in *Geobacter sulfurreducens* biofilms. *Energy Environ. Sci.* **2012**, *5*, 6188−6195.
(45) Zhang, F.; Liu, J.; Ivanov, I.; Hatzell, M. C.; Yang, W.; Ahn, Y.; Logan, B. E. Reference and counter electrode positions affect electrochemical characterization of bioanodes in different bioelectrochemical systems. *Biotechnol. Bioeng.* **2014**, *111*, 1931−1939.
(46) Wang, Z.; Liu, Y.; Li, K.; Liu, D.; Yang, T.; Wang, J.; Lu, J. The influence and mechanism of different acid treatment to activated carbon used as air-breathing cathode catalyst of microbial fuel cell. *Electrochim. Acta* **2017**, *246*, 830−840.
(47) An, J.; Li, N.; Wan, L.; Zhou, L.; Du, Q.; Li, T.; Wang, X. Electric field induced salt precipitation into activated carbon air-cathode causes power decay in microbial fuel cells. *Water Res.* **2017**, *123*, 369−377.
(48) Liu, H.; Cheng, S.; Logan, B. E. Power generation in fed-batch microbial fuel cells as a function of ionic strength, temperature, and reactor configuration. *Environ. Sci. Technol.* **2005**, *39*, 5488−5493.

DOI: 10.1021/acs.est.8b02055
Environ. Sci. Technol. 2018, 52, 8977−8985